

Universität des Saarlandes



Fachrichtung 6.1 – Mathematik

Preprint Nr. 165

**Staircasing in Semidiscrete Stabilised Inverse  
Diffusion Algorithms**

Michael Breuß and Martin Welk

Saarbrücken 2006



# Staircasing in Semidiscrete Stabilised Inverse Diffusion Algorithms

**Michael Breuß**

Technical University Braunschweig  
Carl-Friedrich-Gauß-Faculty of Mathematics and Computer Science  
Computational Mathematics  
Pockelsstraße 14  
38106 Braunschweig  
Germany  
`m.breuss@tu-bs.de`

**Martin Welk**

Mathematical Image Analysis Group  
Faculty of Mathematics and Computer Science  
Saarland University, Bldg. E24  
66041 Saarbrücken  
Germany  
`welk@mia.uni-saarland.de`

Edited by  
FR 6.1 – Mathematik  
Universität des Saarlandes  
Postfach 15 11 50  
66041 Saarbrücken  
Germany

Fax: + 49 681 302 4443  
e-Mail: [preprint@math.uni-sb.de](mailto:preprint@math.uni-sb.de)  
WWW: <http://www.math.uni-sb.de/>

## Abstract

We consider a semidiscrete model problem for the approximation of stabilised inverse linear diffusion processes. The work is motivated by an important observation on fully discrete schemes concerning the so-called staircasing phenomenon: when sharpening monotone data profiles, fully discrete methods generally introduce stepfunction-type solutions reminding of staircases. In this work, we show by an analysis of dynamical systems in corresponding semidiscrete formulations, that already the semidiscrete numerical model contains the relevant information on the occurrence of staircasing. Numerical experiments confirm and complement the theoretical results.

**Keywords:** finite difference methods, stabilised inverse diffusion

**AMS subject classification:** 35M99, 65M06, 65M12

## 1 Introduction

Stabilised inverse linear diffusion (SILD) processes are governed, in a basic formulation, by time-dependent partial differential equations (PDEs) of the form

$$\frac{\partial}{\partial t}u(x, t) = \begin{cases} -c \frac{\partial^2}{\partial x^2}u(x, t) & : \frac{\partial}{\partial x}u(x, t) \neq 0 \\ 0 & : \frac{\partial}{\partial x}u(x, t) = 0 \end{cases}, \quad (1)$$

where  $u$  is a scalar quantity,  $x \in \mathbf{R}$ ,  $t > 0$ , and where  $c > 0$  is a constant anti-diffusion coefficient.

Models of the form (1) are used as sharpening filters within flux-corrected transport (FCT) schemes in the field of computational fluid dynamics [1, 7]. Introduced to image processing in [11], they have also attained fundamental importance as building blocks of image filters, see e.g. [5] and the references therein. Concerning the latter area of application, we mention also [13, 14] where by the name of *stabilised inverse diffusion equations (SIDEs)* a class of nonlinear inverse diffusion processes has been studied.

In this work, we are particularly interested in the analysis of a numerical phenomenon which can spoil the results of SILD filtering, namely the so-called *staircasing phenomenon* [19]: when applied to a strictly monotone data profile, a numerically realised SILD process may generate a stepfunction-type solution reminding of a staircase instead of a new strictly monotone data profile featuring a sharper gradient. Since [19] where staircasing for the Perona–Malik diffusion process [12] was described, it has been observed

in nonlinear diffusion processes involving backward diffusion, see e.g. [16] and references therein. A number of special adaptive diffusion processes have been designed to reduce or avoid staircasing phenomena [3, 6, 10, 16]. However, while algorithmical improvements as those just mentioned have been inspired, the staircasing phenomenon by itself has not been analysed mathematically in much detail up to now.

Recently, it was shown rigorously that the staircasing phenomenon is a common property of numerical solutions obtained by use of *fully discrete schemes* to approximate PDEs of type (1), see [2]. In the context of fully discrete SILD processes, the question arises, if one could avoid staircasing by the choice of a specific time stepping scheme, or, alternatively, by time integration using very small time steps. Furthermore, it is of interest, in order to understand the nature of staircasing as well as a basis for algorithmical developments, whether staircasing events follow a mechanism which can be determined in advance. Coupled with the latter point is the question whether staircasing is a numerically stable phenomenon. In other words: Can small perturbations, caused, e.g., by low-level noise or numerical errors, induce significant changes in the result of a numerical approximation of (1)?

In order to clarify the meaning of these open points, let us briefly discuss fully discrete approximations of (1). To this end, we set  $U_i^n \approx u(i\Delta x, n\Delta t)$  using a space-time grid with corresponding, uniform grid parameters, and denote by  $g_{i\pm 1/2}$  *consistent* numerical fluxes at the boundaries between the cells  $i$  and  $i \pm 1$ , respectively. Then, *consistent* and *conservative* approximations of (1) read

$$U_i^{n+1} = U_i^n - \lambda (g_{i+1/2} - g_{i-1/2}), \quad (2)$$

where  $\lambda := \Delta t/\Delta x$  denotes the ratio of grid parameters. Note that the conservation form respects its divergence form. For stabilisation, we employ the *minmod*-function

$$\text{minmod}(a, b) = \begin{cases} a & : \text{if } a \cdot b > 0 \text{ and } |a| \leq |b| \\ b & : \text{if } a \cdot b > 0 \text{ and } |b| \leq |a| \\ 0 & : \text{else} \end{cases} \quad (3)$$

which can easily be extended to more than two arguments if necessary, compare e.g. [9], by choosing the argument with minimal modulus if the arguments are of the same sign, and zero else. The most basic useful scheme for approximating (1) then incorporates the *minmod* function by

$$g_{i+1/2} = \text{minmod} \left( \frac{1}{\lambda} (U_{i+2}^n - U_{i+1}^n), \frac{c}{\Delta x} (U_{i+1}^n - U_i^n), \frac{1}{\lambda} (U_i^n - U_{i-1}^n) \right). \quad (4)$$

Let us stress, that the natural discretisation of fluxes in (1) is given by means of the middle argument of (4),

$$\frac{c}{\Delta x} (U_{i+1}^n - U_i^n), \quad (5)$$

and its counterpart in  $g_{i-1/2}$ . The other ingredients of  $g_{i\pm 1/2}$  act as stabilisers, which is easily recognised by taking into account the multiplication by  $\lambda$  from (2).

Let us now consider inner points of a strictly monotone data set  $U^0 := \{U_k^0, \dots, U_l^0\}$ . We assume that the extrema  $U_k^0$  and  $U_l^0$  stay fix, and we point out that the events

$$U_{k+1}^{n_1} \equiv U_k^0 \quad \text{or} \quad U_{l-1}^{n_2} \equiv U_l^0 \quad \text{for any } n_1, n_2 \geq 1 \quad (6)$$

are not identical to staircasing as staircasing refers to steps aka constant valued data tuples arising away from extrema. Especially, one may consider to choose the time step size  $\Delta t$  small enough so that the method reduces for many time steps at inner points of  $U^0$  to

$$U_i^{n+1} = U_i^n - \frac{c\Delta t}{\Delta x^2} [(U_{i+1}^n - U_i^n) - (U_i^n - U_{i-1}^n)], \quad i = k+2, \dots, l-2, \quad (7)$$

i.e., in such cases the numerical fluxes reduce to the middle arguments, see (5), so that no stabilisation is taken into account at these points. Heuristically, one then expects that no staircasing occurs in strictly monotone data regimes: numerical fluxes  $g_{i\pm 1/2}$  as in (5) always introduce nonzero updates for  $i = k+2, \dots, l-2$ , for data not distributed exactly along a linear segment where  $U_{i+1}^n - U_i^n = U_i^n - U_{i-1}^n$ . Also the other mentioned aspects of interest are close to this line of argumentation: since one cannot avoid to employ the minmod stabilisation, as is shown in [2], it is natural to assume that the number and position of staircasing artifacts depends on how often the minmod stabilisation takes effect. This frequency in turn could be influenced, e.g., by manipulating the time step size.

Within this paper, we show, that the stated expectations are not based on solid ground. Staircasing arises already in semidiscrete approximations of (1) and is merely bequeathed to fully discrete methods which approximate the semidiscrete process. Concerning the stability question, we show that semidiscrete SILD processes lead to bifurcation problems, so that the stability of numerical results under small data perturbations is not guaranteed for all data configurations. Furthermore, we show that the choice of a time stepping method is not trivial: a naive proceeding can lead to a violation of invariant properties of the semidiscrete formulation of (1), namely that

the total variation as well as the number of extrema of a given signal do not increase during time evolution.

The paper is organised in accordance with the above discussion. Within the next section, the dynamical system arising by semidiscrete methods for the approximation of (1) is analysed in detail, whereby special emphasis is laid on important properties of analytical solutions and their effects with respect to staircasing. Numerical tests demonstrate the validity of the theoretical discussion. The paper is finished with conclusive remarks and acknowledgements.

## 2 Semidiscrete Analysis

### 2.1 The Dynamical System

We consider real-valued, time-dependent signals

$$u = u(t) = (\dots, u_0(t), u_1(t), u_2(t), \dots) \quad (8)$$

of compact support. The latter restriction can be relaxed; it is sufficient to ensure that signals are bounded and do not contain strictly monotone segments of infinite length. Here, we distinguish the time-continuous functions  $u_i(t) \approx u(i\Delta x, t)$  defined at discrete points in space from discrete data  $U_i^n \approx u(i\Delta x, n\Delta t)$  by employing small letters. The parameters  $\Delta x$ ,  $\Delta t$  denote the mesh sizes of a uniform spatial and/or temporal discretisation, respectively. This assumption, too, is not essential and could be relaxed.

Analogously to the proceeding employed in the context of fully discrete formulations, see (2)–(4), a conservative process on a signal (8) can be described by a *dynamical system of ordinary differential equations*

$$\dot{u}_i = \frac{1}{\Delta x} [g_{i-1/2} - g_{i+1/2}], \quad (9)$$

where  $g_{i+1/2} = g_{i+1/2}(u, t)$  is the flux between adjacent *pixels*  $i$  and  $i+1$ . Typically, we assume *translational invariance*, i.e.,  $g_{i+1/2}(u, t) = g_{1/2}(S_{-i}(u), t)$  where  $S_{-i}(u)$  denotes the signal  $u$  shifted by  $-i$  pixels,  $(S_{-i}(u))_j = u_{j+i}$ , and *time-invariance*  $g_{1/2}(u, t) = g_{1/2}(u)$ . The latter assumption means that the system (9) is *autonomous*.

Inverse diffusion without stabilisation can be realised by

$$g_{1/2} = \frac{c}{\Delta x} [-u_0 + u_1], \quad (10)$$

leading to

$$\dot{u}_i = \frac{c}{\Delta x^2} [-u_{i-1} + 2u_i - u_{i+1}]. \quad (11)$$



A *stabilisation* is introduced in order to ensure that local extrema become invariant values, compare also the discussion in [2] for the fully discrete case. This means, that (10) is used only if neither  $u_0$  nor  $u_1$  is an extremum, otherwise we set  $g_{1/2} = 0$ .

The stabilised version of (11) thus reads as the system

$$\dot{u}_i = \frac{c}{\Delta x^2} \begin{cases} (-u_{i-1} + 2u_i - u_{i+1}) & : (u_{i-2}, u_{i-1}, u_i, u_{i+1}, u_{i+2}) \\ & \text{strictly monotone} \\ (u_i - u_{i+1}) & : (u_{i-1}, u_i, u_{i+1}, u_{i+2}) \text{ strictly monotone} \\ & \text{and } u_{i-1} \text{ local extremum} \\ (-u_{i-1} + u_i) & : (u_{i-2}, u_{i-1}, u_i, u_{i+1}) \text{ strictly monotone} \\ & \text{and } u_{i+1} \text{ local extremum} \\ 0 & : \text{ else.} \end{cases} \quad (12)$$

Herein, a local extremum is understood as any pixel  $u_i$  for which the sequence  $(u_{i-1}, u_i, u_{i+1})$  is not strictly monotone. For instance, in the sequence  $u_0 > u_1 = u_2 > u_3$  both  $u_1$  and  $u_2$  are local extrema.

The equations (12) comprise a dynamical system with discontinuous right-hand side. It is therefore necessary to specify the concept of solution. This technique is studied in greater generality, e.g., in [4], and it has been applied in the context of image filters, e.g., in [15, 17].

Given an initial signal  $(\dots, f_0, f_1, f_2, \dots)$ , we say that a time-dependent signal  $(\dots, u_0(t), u_1(t), u_2(t), \dots)$  is a solution of the initial-value problem consisting of the differential equations (12) and the initial conditions

$$u_i(0) = f_i, \quad i = \dots, 0, 1, 2, \dots, \quad (13)$$

if

- (I) each  $u_i$  is a continuous, piecewise differentiable function of  $t$ ,
- (II) each  $u_i$  satisfies (12) for all  $t$  for which  $\dot{u}_i(t)$  exists,
- (III) for  $t = 0$ , the right-sided derivative  $\dot{u}_i^+(0)$  equals the right-hand side of (12).

Having thus explained what we understand by a solution of (12), we will refer in the following to (12) as *semidiscrete stabilised inverse linear diffusion*.

## 2.2 Analytical Solution

Throughout the remainder of Section 2 we set for simplicity  $\Delta x = 1$ ,  $c = 1$ , since this does not influence any structural assertion. We note first the following facts.

**Lemma 2.1** *Let  $(\dots, u_0(t), u_1(t), u_2(t), \dots)$  be a solution of (12)–(13) in the sense of (I)–(III).*

*Then the following hold:*

1. *If  $u_i$  is a local extremum at a time  $t = t_0$ , its neighbours  $u_{i-1}$  and  $u_{i+1}$  can not move away from  $u_i$  at  $t = t_0$ .*
2. *If  $u_i$  is a local extremum at a time  $t_0$ , it remains a local extremum for all  $t > t_0$ .*
3. *If  $u_i = u_{i+1}$  at a time  $t_0$ , then the same equality holds for all  $t > t_0$ .*

*Remark.* The Lemma implies particularly the preservation of monotonicity, thereby guaranteeing that the process is *total variation preserving (TVP)*, compare [9] for this notion.

**Proof.** We prove that, as long as  $u_i$  is a local extremum, its neighbour  $u_{i+1}$  can move only towards  $u_i$ . Indeed, in case  $u_i$  is a local extremum we have, see (12),

$$\dot{u}_{i+1} = \begin{cases} (u_{i+1} - u_{i+2}) & \text{if neither } u_{i+1} \text{ nor } u_{i+2} \text{ is a local extremum,} \\ 0 & \text{else.} \end{cases} \quad (14)$$

If thus  $\dot{u}_{i+1}$  is to be non-zero,  $u_{i+1}$  cannot be an extremum, and  $u_{i+1} - u_i$  and  $u_{i+2} - u_{i+1}$  have the same sign. Consequently,

$$\text{sgn}(\dot{u}_{i+1}) = \text{sgn}(u_i - u_{i+1}) \quad (15)$$

holds at any time  $t$  in case  $u_i$  is an extremum. Note, that the left neighbour  $u_{i-1}$  of  $u_i$  can be treated in an analogous fashion. This proves the first statement.

Next, we want to prove that pixels, once they have attained the same value, cannot split up again to attain different values. Assume there were two neighbouring pixels  $u_i$  and  $u_{i+1}$  which are equal at time  $t_0$  and unequal at time  $t_1 > t_0$ , without loss of generality we set  $u_{i+1}(t_1) > u_i(t_1)$ . Furthermore, we assume that the interval  $(t_0, t_1)$  is chosen such that the signs of differences  $u_{i+2} - u_{i+1}$  and  $u_{i-1} - u_i$  do not change within the interval, and such that

$u_i$  and  $u_{i+1}$  are differentiable throughout the interval  $(t_0, t_1)$ . Note that this can always be ensured by splitting the interval if necessary. According to the mean-value theorem of differential calculus, there exists a  $\vartheta \in (t_0, t_1)$  such that

$$(t_1 - t_0)(\dot{u}_{i+1}(\vartheta) - \dot{u}_i(\vartheta)) = (u_{i+1}(t_1) - u_i(t_1)) - (u_{i+1}(t_0) - u_i(t_0)), \quad (16)$$

i.e., we must have that  $\dot{u}_{i+1}(\vartheta) - \dot{u}_i(\vartheta) > 0$ .

If  $u_i$  is a local minimum at  $t = \vartheta$  (thus, throughout  $(t_0, t_1)$ ), we have that  $u_{i+1}$  is not an extremum, and it follows that

$$\dot{u}_{i+1}(\vartheta) - \dot{u}_i(\vartheta) = u_{i+1} - u_{i+2} < 0. \quad (17)$$

An analogous argument holds if  $u_{i+1}$  is a local maximum and  $u_i$  not an extremum.

Finally, if neither  $u_i$  nor  $u_{i+1}$  is an extremum at  $t = \vartheta$ , we have that  $u_{i-1} - u_i, u_i - u_{i+1}, u_{i+1} - u_{i+2}$  are all negative in  $(t_0, t_1)$ , and at least one of  $u_{i-1} - u_i, u_{i+1} - u_{i+2}$  is negative for  $t = t_0$ . By choosing the interval  $(t_0, t_1)$  small enough, we can achieve that  $2(u_i - u_{i+1}) > u_{i-1} - u_i + u_{i+1} - u_{i+2}$  throughout  $(t_0, t_1)$ , from which it follows that

$$\dot{u}_{i+1}(\vartheta) - \dot{u}_i(\vartheta) = (u_{i+1} - u_{i+1}) - 2(u_i - u_{i+1}) + (u_{i-1} - u_i) < 0. \quad (18)$$

In all cases we have therefore obtained a contradiction to (16), which proves the second statement of our lemma.

The third assertion follows from the fact that for a local extremum to lose its extremality, it would have to be “passed” by one of its neighbours, which would therefore have to be equal to the extremum at some time (remember  $u$  is continuous with respect to  $t$ ). According to the second statement, the two pixels would irreversibly merge in this case.  $\square$

It is therefore sufficient to consider the evolution of signal segments of finite length whose first and last pixels are local extrema, and which are strictly monotone. Without loss of generality, we consider a decreasing segment  $f_0 > f_1 > \dots > f_n > f_{n+1}$  where  $f_0$  is a local maximum and  $f_{n+1}$  a local minimum. Thus, we have the evolution equations

$$\left. \begin{aligned} \dot{u}_0 &= 0, \\ \dot{u}_1 &= u_1 - u_2, \\ \dot{u}_i &= -u_{i-1} + 2u_i - u_{i+1}, \quad 2 \leq i \leq n-1, \\ \dot{u}_n &= -u_{n-1} + u_n, \\ \dot{u}_{n+1} &= 0, \end{aligned} \right\} \quad (19)$$

which hold throughout any time interval  $(0, T)$  in which  $u_0 > u_1 > \dots > u_n > u_{n+1}$  stays true.

The system (19) is a system of linear ODEs which can be solved analytically. Leaving aside  $u_0$  and  $u_{n+1}$ , we can rewrite the system for  $\mathbf{u} := (u_1, \dots, u_n)^\top$  as

$$\dot{\mathbf{u}} = A\mathbf{u} \quad (20)$$

with the  $n \times n$  matrix

$$A = \begin{pmatrix} 1 & -1 & 0 & \dots & \dots & 0 \\ -1 & 2 & -1 & 0 & & 0 \\ 0 & -1 & 2 & -1 & 0 & 0 \\ \vdots & & \ddots & \ddots & \ddots & \vdots \\ 0 & \dots & 0 & -1 & 2 & -1 \\ 0 & \dots & \dots & 0 & -1 & 1 \end{pmatrix}. \quad (21)$$

The matrix  $A$  is positive semidefinite, since Gershgorin's Theorem ensures all eigenvalues to be nonnegative. Moreover,  $A$  has rank  $n - 1$  since it contains a triangular  $(n - 1) \times (n - 1)$  submatrix without zeros on its diagonal. We simplify therefore the system by eliminating the zero eigenvalue and corresponding eigenvector.

For  $v_0 := \frac{1}{\sqrt{n}} \sum_{i=1}^n u_i$  we have  $\dot{v}_0 = 0$ , implying  $v_0(t) = v_0(0)$  for all  $t$ . In fact,  $v_0 = a_0^\top \mathbf{u}$  where  $a_0 = \frac{1}{\sqrt{n}}(1, \dots, 1)^\top$  is the eigenvector with eigenvalue zero of  $A$ .

Let us now set  $v_i := u_i - u_{i+1}$ ,  $i = 1, \dots, n - 1$ , and  $\mathbf{v} := (v_1, \dots, v_{n-1})^\top$ , i.e.,

$$\mathbf{v} := D\mathbf{u}, \quad (22)$$

with the  $(n - 1) \times n$  matrix

$$D = \begin{pmatrix} 1 & -1 & 0 & \dots & 0 \\ 0 & 1 & -1 & 0 & 0 \\ \vdots & & \ddots & \ddots & \\ 0 & \dots & 0 & 1 & -1 \end{pmatrix}. \quad (23)$$

Introducing additionally the  $(n - 1) \times (n - 1)$  matrix

$$B = \begin{pmatrix} 2 & -1 & 0 & \dots & \dots & 0 \\ -1 & 2 & -1 & 0 & & 0 \\ 0 & -1 & 2 & -1 & 0 & 0 \\ \vdots & & \ddots & \ddots & \ddots & \vdots \\ 0 & \dots & 0 & -1 & 2 & -1 \\ 0 & \dots & \dots & 0 & -1 & 2 \end{pmatrix}, \quad (24)$$

one easily sees that

$$D^T D = A, \quad D D^T = B . \quad (25)$$

Thus, by (20) and (25), we obtain

$$D \dot{\mathbf{u}} = D A \mathbf{u} = B D \mathbf{u} , \quad (26)$$

i.e., a new linear dynamical system for  $\mathbf{v}$ :

$$\dot{\mathbf{v}} = B \mathbf{v} . \quad (27)$$

The analytical solution of (27) is given by

$$\mathbf{v}(t) = e^{Bt} \mathbf{v}(0) \quad (28)$$

which we will make more explicit using the eigendecomposition of the symmetric matrix  $B$ .

**Lemma 2.2** *Let  $\delta_k := \pi k/n$ . Then*

$$b_k := \sqrt{\frac{2}{n}} (\sin(\delta_k), \sin(2\delta_k), \dots, \sin((n-1)\delta_k))^T \quad (29)$$

for  $k = 1, \dots, n-1$  are normalised eigenvectors of  $B$ , with corresponding eigenvalues

$$\lambda_k = 2(1 - \cos(\delta_k)) . \quad (30)$$

*Remark.* The matrix  $B$  represents a discrete Laplacian with zero boundary conditions. Consequently, its eigenvectors are discretised harmonic functions, namely the basis of a discrete sine transform.

**Proof.** By direct calculation one checks that each  $b_k$  is of unit length and satisfies

$$B b_k = 2(1 - \cos(\delta_k)) b_k . \quad (31)$$

□

Via

$$\mathbf{v}(t) = \sum_{k=1}^{n-1} \langle b_k, \mathbf{v}(0) \rangle b_k e^{\lambda_k t} \quad (32)$$

we can rewrite (28) to obtain directly the following statement.

**Proposition 2.3** *For  $t \in [0, T]$  the solution of (27) is given by*

$$v_i(t) = \frac{2}{n} \sum_{j=1}^{n-1} \left( \sum_{k=1}^{n-1} \sin \frac{\pi i k}{n} \sin \frac{\pi j k}{n} e^{2\left(1 - \cos \frac{\pi k}{n}\right)t} \right) v_j(0) . \quad (33)$$

The analytical solution of (20) is then computed by backsubstituting  $u$  for  $v$  and it is given within the following corollary.

**Corollary 2.4** *The solution of (20) for  $t \in [0, T]$  is given by*

$$u_i(t) = \frac{1}{n} \left( \sum_{j=1}^n u_j(0) - \sum_{j=1}^{i-1} j v_j(t) + \sum_{j=i}^{n-1} (n-j) v_j(t) \right), \quad (34)$$

where  $v_j(t)$  are given by (33), and thus by

$$u_i(t) = \sum_{j=1}^n \left( \frac{1}{n} + \frac{4}{n^2} \sum_{k=1}^{n-1} \cos \frac{\pi(2j-1)k}{2n} \sin \frac{\pi k}{2n} e^{2(1-\cos \frac{\pi k}{n})t} \times \right. \\ \left. \times \left( \sum_{l=1}^{n-1} l \sin \frac{\pi l k}{n} + n \sum_{l=i}^{n-1} \sin \frac{\pi l k}{n} \right) \right) u_j(0). \quad (35)$$

In (34) and (35), sums with upper limit below lower limit are to be read as zero.

*Remark.* The evolution (20) (or also (35)) can also be read as non-stabilised inverse linear diffusion on a finite signal  $(u_1, \dots, u_n)$  with reflecting, i.e., zero-flux, boundary conditions. That is to say, in time intervals between pixel merging events the strictly monotone segments of semidiscrete stabilised inverse linear diffusion follow an ordinary inverse linear diffusion dynamics; at merging events, just the segmentation changes.

## 2.3 Staircasing in Segments

We continue considering a strictly decreasing signal segment enclosed between two local extrema, and we want to determine under which conditions staircasing occurs. We start with the following observation.

**Lemma 2.5** *Let a strictly decreasing segment  $(f_0, \dots, f_{n+1})$  with local extrema  $f_0$  and  $f_{n+1}$  be given,  $n \geq 2$ , and let  $(u_0, \dots, u_{n+1})$  evolve according to (12) with initial condition  $u(0) = f$ . Then the dynamics of  $(u_1, \dots, u_n)$  follows (20) until one of the following events happens:*

- (a) *One of the pixels  $u_1, u_n$  merges with its extremal neighbour pixel  $u_0, u_{n+1}$ , respectively.*
- (b) *Two neighbouring pixels  $u_i, u_{i+1}$  ( $1 \leq i \leq n-1$ ) become equal.*

*Either (a) or (b) occurs for a finite  $t = T$ .*

Case (b) describes a staircasing event, entailing a transition to two smaller segments, while in case (a) a transition to a smaller segment takes place without staircasing. Even in the latter case, a later staircasing event involving the same pixels is still possible but then governed by the dynamics of the new segments.

**Proof.** It is clear that the dynamics (20) is terminated as soon as (a) or (b) occurs. It remains to show that whatever initial values are given, this happens at finite evolution time  $t = T$ .

From Lemma 2.1 it follows that for  $n \geq 2$  both  $u_1$  and  $u_n$  evolve in direction of their neighbouring extrema as long as no staircasing involving these pixels has occurred, i.e.,  $u_1 > u_2$  and  $u_{n-1} > u_n$  hold. From (33) which contains only exponential summands with positive exponents it is clear that the velocity of both pixels cannot go asymptotically to zero; thus, whatever values  $u_0$  and  $u_{n+1}$  might have (which don't influence the dynamics of  $u_1, \dots, u_n$  directly), either  $u_1$  or  $u_n$  will merge with its neighbouring extremum in finite time.  $\square$

However, by choosing  $f_0$  large enough and  $f_{n+1}$  small enough, the end-of-segment merging events can be pushed to arbitrarily large values of  $t$ . This leads us to ask: *For which values of  $u_1, \dots, u_n$  is the dynamics (20) guaranteed to be terminated by an end-of-segment merging event of type (a), independent on  $f_0$  and  $f_{n+1}$ ?*

To answer this question, we consider the dynamics (20) just as ordinary semidiscrete inverse diffusion with zero-flux boundary conditions, and focus on the differences  $v_1, \dots, v_{n-1}$ . These differences are positive at  $t = 0$ , and staircasing events are indicated by at least one of these differences reaching zero. We can then prove the following result.

**Proposition 2.6** *Given a strictly decreasing signal  $(f_1, \dots, f_n)$ , the dynamics (20) with initial condition  $u(0) = f$  preserves the strict monotonicity  $u_1 > \dots > u_n$  for all  $t > 0$  if and only if the differences  $v_1(0) = f_1 - f_2, \dots, v_{n-1}(0) = f_{n-1} - f_n$  are given by some multiple  $\mu b_1$  of the eigenvector  $b_1$  with  $\mu > 0$ .*

The proof relies on two important properties of the eigendecomposition of  $B$  which can be directly read off the formulae (29), (30).

**Lemma 2.7** *For the eigenvectors and eigenvalues of  $B$  given by (29), (30), the following properties hold:*

1. *The eigenvalues are ordered by size,  $\lambda_1 < \lambda_2 < \dots < \lambda_{n-1}$ .*

2. *Exactly one eigenvector, namely  $b_1$  which corresponds to the smallest eigenvalue, has only positive components. Each of the eigenvectors  $b_2, \dots, b_{n-1}$  has at least one negative component.*

**Proof of Proposition 2.6.** Since  $\mathbf{v}(0)$  has positive components,  $\langle \mathbf{v}(0), b_k \rangle \neq 0$  holds for some  $k$ . Let  $k$  be the largest index with this property. Considering (32) for  $t \rightarrow \infty$ , we have that

$$\lim_{t \rightarrow \infty} \frac{\mathbf{v}(t)}{e^{2\lambda_k t}} = \langle \mathbf{v}(0), b_k \rangle b_k . \quad (36)$$

Assuming that  $v_i > 0$  for all  $i$  and all  $t$ , the limits on the left hand side of (36) must be nonnegative which can only be the case if all components of  $b_k$  are nonnegative, or if all are nonpositive. According to Lemma 2.7 this implies  $k = 1$ .  $\square$

Initial values  $f$  which do not satisfy the condition from Proposition 2.6 can be classified depending on which neighbouring values in the signal will merge first. We describe this classification qualitatively in terms of the difference variables  $\mathbf{v}$ .

To this end, we note that (28) can be evaluated for negative  $t$  as well as for positive  $t$  since the linear system (27) is *reversible*, implying, that all initial values  $\mathbf{v}^\circ$  which lead to a certain state  $\mathbf{v}^*$  later on can also be obtained by (28) if  $\mathbf{v}(0) = \mathbf{v}^*$  is used as an initial condition and going backwards in time. Since we seek to investigate which  $v_i$  vanishes first during evolution, we want to know *where* trajectories leave the sector  $(\mathbb{R}_0^+)^{n-1}$ . The boundary of this sector is made up by  $n - 1$  *facets*, each of them characterised by one of the variables  $v_i$ ,  $i \in \{1, \dots, n - 1\}$  attaining zero value. Let the facet consisting of all these points  $(v_0 > 0, \dots, v_i = 0, \dots, v_{n-1} > 0)^T$  be denoted by  $S_i$ . Each facet is simply connected. Denoting by  $T_{t < 0}(\mathbf{v})$  the trajectory of a point  $\mathbf{v} \in \mathbb{R}^{n-1}$  propagating under (28) backwards in time, we see that the set of initial conditions for which  $v_i$  is the first variable to vanish during evolution is exactly

$$T_{t < 0}(S_i) := \bigcup_{\mathbf{v} \in S_i} T_{t < 0}(\mathbf{v}) . \quad (37)$$

Note that solutions of (28) are continuous in  $t$ . Moreover, they depend continuously on initial conditions, and because of the reversibility of the system, trajectories are either identical or disjoint. The union  $T_{t < 0}(S_i)$  of negative trajectories starting on a single facet  $S_i$  is therefore a simply connected  $(n - 1)$ -dimensional point set in  $\mathbb{R}^{n-1}$ , whose boundary consists of the facet  $S_i$  itself and those trajectories starting on the boundary of  $S_i$ ,

$$\partial T_{t < 0}(S_i) = S_i \cup T_{t < 0}(\partial S_i) . \quad (38)$$



Different sets  $T_{t<0}(S_i)$ ,  $T_{t<0}(S_j)$  are therefore separated by hypersurfaces  $T_{t<0}(S_{ij})$ ,  $S_{ij} := \partial S_i \cap \partial S_j$  (except for  $n = 3$  where the separating line cannot be obtained from  $S_{12} = \{0\}$  in this way, see instead the discussion below for this case). The topology of the resulting separation of  $(\mathbb{R}_0^+)^{n-1}$  is therefore equivalent to the topology of the  $(n-1)$ -dimensional surface of a  $n$ -dimensional (hyper)cube corner.

We notice further that if  $\mathbf{v} \in T_{t<0}(S_i)$ , then the linearity of (28) implies  $\alpha \mathbf{v} \in T_{t<0}(S_i)$  for any  $\alpha > 0$ . This ensures that any hyperplane  $H = H_{\mathbf{n},C}$  defined by  $\langle \mathbf{n}, \mathbf{v} \rangle = C$  (where  $\langle \cdot, \cdot \rangle$  denotes Euclidean scalar product,  $\mathbf{n} \in (\mathbb{R}_0^+)^{n-1}$  and  $C > 0$  are fixed) is transversal to all trajectories under consideration. Thus, the separation of  $(\mathbb{R}_0^+)^{n-1}$  induces by restriction a separation of  $(\mathbb{R}_0^+)^{n-1} \cap H$  whose topology equals that of the  $(n-2)$ -dimensional surface of a  $(n-1)$ -dimensional (hyper)cube corner.

We discuss the simplest cases explicitly.

*Case  $n = 2$ .* Since  $B$  is a scalar, all initial values satisfy the conditions of Proposition 2.6, i.e., no staircasing takes place.

*Case  $n = 3$ .* The sets  $T_{t<0}(S_1)$  and  $T_{t<0}(S_2)$  are separated by a line which due to symmetry considerations and because of the scaling property  $\alpha T_{t<0}(S_i) = T_{t<0}(S_i)$  must be the bisector of the quadrant  $(\mathbb{R}_0^+)^2$ , i.e.,  $v_1 = v_2$ . Initial values with  $v_1(0) > v_2(0)$  make  $v_2$  vanish first, others with  $v_1(0) < v_2(0)$  make  $v_1$  vanish first.

*Case  $n = 4$ .* The three facets  $S_1, S_2, S_3$  bounding the octant  $(\mathbb{R}_0^+)^3$  share the boundary half-lines  $S_{12} = \{(0, 0, a)^T \mid a \geq 0\}$ ,  $S_{13} = \{(0, a, 0)^T \mid a \geq 0\}$ ,  $S_{23} = \{(a, 0, 0)^T \mid a \geq 0\}$ , respectively. Inserting  $(0, 0, a)^T$  into (28) gives

$$\left. \begin{aligned} v_1(t) &= \frac{1}{2} \left( \frac{1}{2} e^{(2-\sqrt{2})t} - e^{2t} + \frac{1}{2} e^{(2+\sqrt{2})t} \right) a \\ v_2(t) &= \frac{1}{2} \left( \frac{\sqrt{2}}{2} e^{(2-\sqrt{2})t} - \frac{\sqrt{2}}{2} e^{(2+\sqrt{2})t} \right) a \\ v_3(t) &= \frac{1}{2} \left( \frac{1}{2} e^{(2-\sqrt{2})t} + e^{2t} + \frac{1}{2} e^{(2+\sqrt{2})t} \right) a \end{aligned} \right\} \quad (39)$$

which by the substitution

$$\alpha := \frac{1}{4} e^{2t} (e^{t\sqrt{2}/2} + e^{-t\sqrt{2}/2})^2, \quad \beta := \frac{e^{t\sqrt{2}/2} - e^{-t\sqrt{2}/2}}{e^{t\sqrt{2}/2} + e^{-t\sqrt{2}/2}} \quad (40)$$

simplifies to

$$v_1(t) = \alpha \beta^2, \quad v_2(t) = \sqrt{2} \alpha \beta, \quad v_3(t) = \alpha. \quad (41)$$

Taking into account that  $a > 0$  and  $t < 0$ , it follows that

$$T_{t<0}(S_{12}) = \{(\alpha\beta^2, \sqrt{2}\alpha\beta, \alpha)^T \mid \alpha > 0, 0 < \beta < 1\}. \quad (42)$$

Analogous considerations lead to

$$\left. \begin{aligned} T_{t<0}(S_{23}) &= \{(\alpha, \sqrt{2}\alpha\beta, \alpha\beta^2)^T \mid \alpha > 0, 0 < \beta < 1\} \\ T_{t<0}(S_{13}) &= \{(\alpha, \sqrt{2}\beta, \alpha)^T \mid 0 < \alpha < \beta\} \end{aligned} \right\} \quad (43)$$

which finally allow us to establish the following set of criteria, for given initial values  $\mathbf{v}(0) = (v_1(0), v_2(0), v_3(0))^T$ :

$$\left. \begin{aligned} v_2(0) < \sqrt{2v_1(0)v_3(0)} &\Rightarrow v_2 \text{ vanishes first,} \\ v_2(0) > \sqrt{2v_1(0)v_3(0)} \text{ and } v_1(0) < v_3(0) &\Rightarrow v_1 \text{ vanishes first,} \\ v_2(0) > \sqrt{2v_1(0)v_3(0)} \text{ and } v_1(0) > v_3(0) &\Rightarrow v_3 \text{ vanishes first.} \end{aligned} \right\} \quad (44)$$

### 3 Numerical tests

Within this section, we follow two topics of interest. At first, we validate experimentally the bifurcation results from the preceding paragraph, thus showing that staircasing is predictable by theory. Note, that the test data are chosen so that the experiments featuring staircasing can be understood as perturbed data of the non-staircasing test case, thus showing that data perturbations, e.g. due to low-level noise or preceding numerical errors in the case of FCT schemes, may influence the outcome of a SILD process. Complementing these investigations, we discuss the influence of time stepping schemes by use of a numerical staircase-type solution.

#### 3.1 Validation of semidiscrete theory

In order to validate the results of our bifurcation analysis, we consider a couple of data segments of length  $n = 4$  which can be classified according to Proposition 2.6 and (44), respectively. As the theoretical results are obtained for the semidiscrete case, we integrate in time using Euler forward time stepping with very small time step sizes, i.e., we generally use  $\Delta t = 10^{-7}$ . For easy reference within given figures, we use  $\Delta x = 1$  as within the theoretical discussion.

### Case 1 – no staircasing

We consider the following set of initial data:

$$\{U_0^0, U_1^0, U_2^0, U_3^0, U_4^0, U_5^0\} = \{2, 1.1707, 1.0707, 0.9293, 0.8293, 0\}, \quad (45)$$

continued by constant states  $U_i^0 = 2$ ,  $i < 0$ , and  $U_i^0 = 0$ ,  $i > 5$ , respectively. Taking into account Proposition 2.6, we observe that the data (45) correspond to  $v_1 = v_3$  and  $v_2 = \sqrt{2}v_1$ . Within Figure 1 (top, left) we display the initial signal as well as its steady state solution, evaluated at  $t = 3$ . As predicted, there is no visible staircasing effect.

### Case 2 – staircasing in the middle of a profile

For this test case, we consider the set of initial data reading:

$$\{U_0^0, U_1^0, U_2^0, U_3^0, U_4^0, U_5^0\} = \{2, 1.16, 1.06, 0.94, 0.84, 0\}, \quad (46)$$

continued as in the preceding test case by constant states left and right. As easily observed, this case corresponds to  $v_2 < \sqrt{2v_1v_3}$ . Let us again emphasise, that the data from (46) differ only marginally from signal (45). Within Figure 1 (top, right) we show the initial signal as well as its steady state solution, evaluated again at  $t = 3$ . As predicted, staircasing is observable at the middle of the profile, with  $U_2^k = U_3^k = 1$  for large  $k$ .

### Case 3 – staircasing at an end of a profile

For this test case, we consider the set of initial data incorporating:

$$\{U_0^0, U_1^0, U_2^0, U_3^0, U_4^0, U_5^0\} = \{2, 1.1707, 1.0807, 0.9393, 0.8293, 0\}. \quad (47)$$

Also here, let us note, that (47) is very close to signal (45); one can easily verify for this case  $v_2 > \sqrt{2v_1v_3}$  and  $v_1 < v_3$ .

The initial signal as well as two states of interest are shown in Figure 1 (bottom row). At  $t = 1.8$ , we observe as predicted that staircasing occurs first near the left end of the profile. The steady state solution then is dominated by the first staircasing event.

*Remark.* The case that  $v_3$  vanishes first, see (44), can be realised numerically in an analogous fashion.

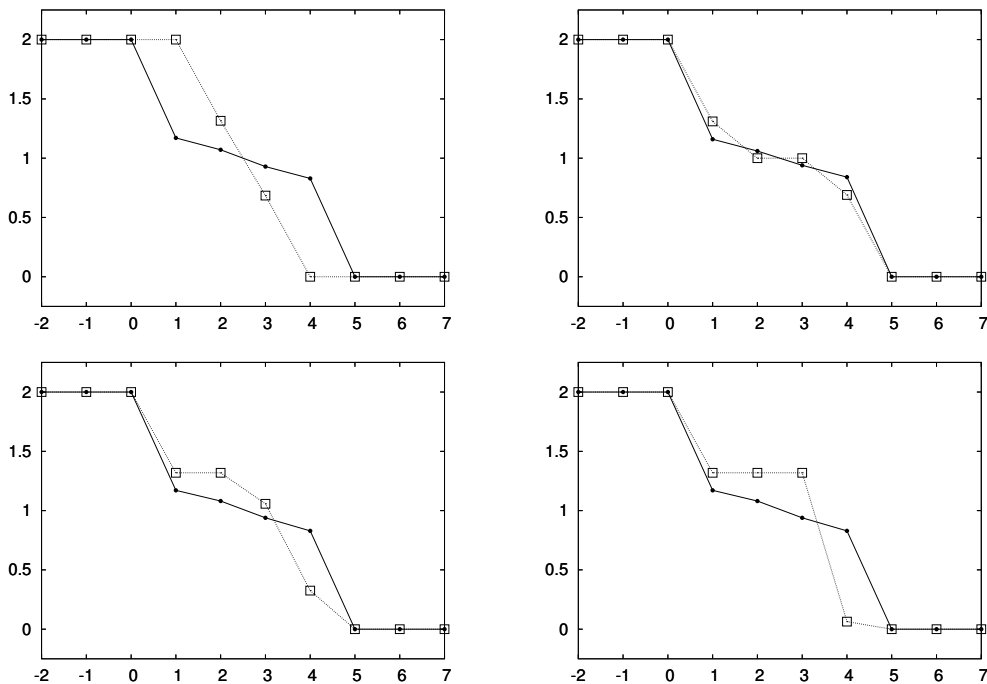


Figure 1: Initial states (lines with dots) together with numerical states (squares), as described below. **Top left:** initial signal from (45) and steady state without staircasing. **Top right:** initial data from (46) and steady state featuring staircasing at the middle of the profile. **Bottom row:** initial state from (47), as well as **(left)** intermediate state with staircasing at an end of the profile, **(right)** steady state dominated by previous staircasing.

### 3.2 Discussion of time integration

In this section, we want to investigate experimentally the influence of time discretisation methods on a stable situation away from a bifurcation situation, thus complementing the above numerical tests.

To this end, we employ a useful academic test case, i.e., we are concerned with a variation of the *tent function* already suggested in [2], here given as an initial function  $u_0$ :

$$u_0(x) = \begin{cases} \alpha \sin\left(\frac{\pi}{2}(x+1)\right) + \beta & : -\frac{1}{2} \leq x \leq \frac{1}{2} \\ 0 & : \text{else} \end{cases}. \quad (48)$$

Setting  $\alpha = 5$  and  $\beta = 0$ , we obtain on a grid with  $\Delta x = 0.1$  the function  $u_0$  together with its discrete representation displayed in Figure 2 (left). Evidently, the discretisation is quite coarse; however, as already exemplified in

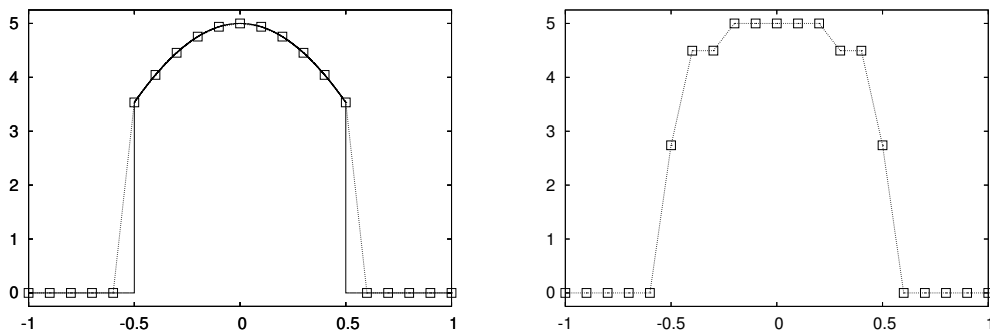


Figure 2: **Left:** analytic (line) and discrete (squares) initial states. **Right:** staircasing by propagation of discrete initial state.

[2], all phenomena observable on a coarse grid are also observable when using a fine spatial resolution.

Taking the discrete data displayed in Figure 2 (left) and doing 8 time steps with  $\Delta t = 0.002$  using the *fully discrete* method from (2)–(4), we obtain the staircasing situation given in Figure 2 (right). Since the discretisation error of the time stepping scheme in use, which is, as easily seen,  $O(\Delta t)$ , implies that one obtains in the limit  $\Delta t \downarrow 0$  the semidiscrete scheme (9), we ask for the numerical results we obtain by re-computing the situation given in Figure 2 (right) using very small time step sizes. In Figure 3, we show the computational results employing  $1.6 \cdot 10^5$  time steps with  $\Delta t = 10^{-7}$ , and  $1.6 \cdot 10^7$  time steps with  $\Delta t = 10^{-9}$ , respectively. We observe nearly the same staircase-like structure as in the case of the coarse time discretisation, see Figure 2 (right); the differences of the employed time step sizes are observable only by the slightly more rounded structure of the signals in Figure 3 compared with Figure 2 (right). Here, as staircasing is an unquestioned feature of the spatial discretisation, the error of the time discretisation takes the role of an approximation error resulting in a slightly rougher profile. However, as it is clear after our discussion, staircasing cannot be avoided.

We now want to point out here a difference between the fully discrete method employing the Euler time stepping method, (2)–(4), and the semidiscrete methods: in the fully discrete case there exist data constellations circumventing the effect of merging events aka, in the semidiscrete form, the minmod stabilisation. In order to show this, we modify the case discussed above by choosing  $\alpha = 5$  and  $\beta = -5/2$ ; thus, we translate the tent function from Figure 2 (left) a bit into negative  $y$ -direction, see Figure 4 (left); note the new scaling of the  $y$ -axis. Doing then 9 time steps with  $\Delta t = 0.001$ , we observe that slight new extrema are produced, see Figure 4 (right). The

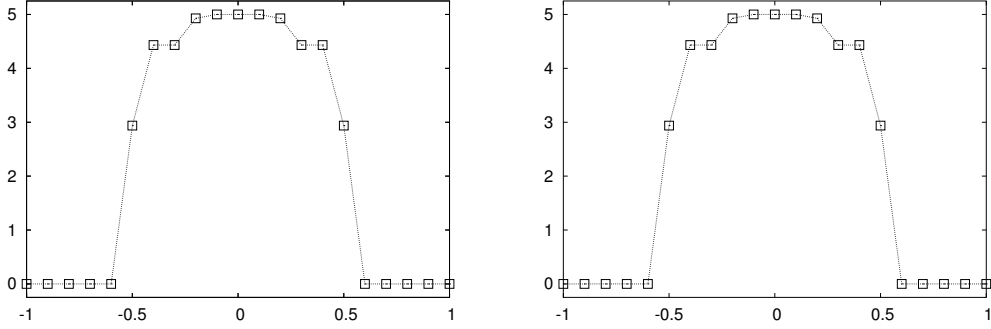


Figure 3: Re-computations of staircasing solutions. **Left:** using  $1.6 \cdot 10^5$  time steps with  $\Delta t = 10^{-7}$ . **Right:** using  $1.6 \cdot 10^7$  time steps with  $\Delta t = 10^{-9}$ .

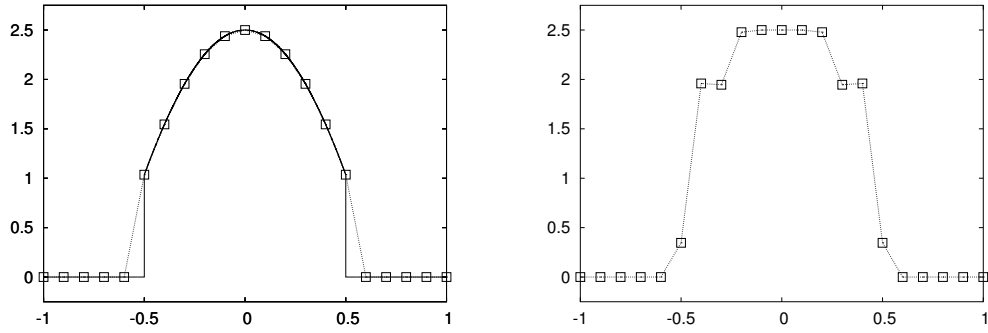


Figure 4: **Left:** analytic (line) and discrete (squares) initial states. **Right:** numerical solution (and steady state) after 9 time steps with slight new extrema.

reason for this at first glance unusual behaviour is, that at the critical points where new extrema arise the method is reduced at the ninth time step to scheme (7), i.e., the stabilisation has taken no effect, which is impossible in the semidiscrete case.

Let us stress, that the latter experiment shows that important qualities of the semidiscrete method are not taken over to the fully discrete case: the TVP property is violated, as the new extrema shown in Figure 4 increase the total variation of the initial signal. Note also, that the fact that the number of extrema is not preserved in our example is an important point to notice with respect to FCT schemes for conservation laws, compare [8].

As a possible remedy, one could modify the numerical flux (4) as

$$g_{i+1/2} = \text{minmod} \left( \frac{1}{2\lambda}(U_{i+2}^n - U_{i+1}^n), \frac{c}{\Delta x}(U_{i+1}^n - U_i^n), \frac{1}{2\lambda}(U_i^n - U_{i-1}^n) \right), \quad (49)$$

thus restricting the updates of variables within one time step of the fully discrete scheme in such a way that none of two neighbouring pixels is allowed to travel more than half the distance towards its neighbour. This is in fact the same sort of stability limit as used in the 1-D total variation diffusion scheme of [15]. A disadvantage from the theoretical point of view could be that neighbouring pixels approach each other only asymptotically, thus postponing the actual merging events from *finite* to *infinite* times. This happens also in the semidiscrete shock filter scheme in [17], discussed in more detail in [18].

Another possible remedy is based on the observation that it requires two adjacent data moving in opposite directions to generate a new extremum. Transferring the procedure described in [18] we obtain a two-step TVP scheme:

*Step 1*

$$\tilde{U}_i^n = U_i^n - \lambda(g_{i+1/2} - g_{i-1/2}). \quad (50)$$

*Step 2*

$$U_i^{n+1} = \begin{cases} \frac{1}{2}(\tilde{U}_{i+1}^n + \tilde{U}_i^n) & : (\tilde{U}_{i+1}^n - \tilde{U}_i^n)(U_{i+1}^n - U_i^n) < 0 \\ \frac{1}{2}(\tilde{U}_{i-1}^n + \tilde{U}_i^n) & : (\tilde{U}_{i-1}^n - \tilde{U}_i^n)(U_{i-1}^n - U_i^n) < 0 \\ \tilde{U}_i^n & : \text{else} \end{cases} \quad (51)$$

These steps substitute (2), while retaining (4). Note, that the modification by (50)–(51) is conservative as data at (automatically adjacent) new extrema are replaced by their average.

It also is important to note that both schemes, (2) with (49) as well as (50)–(51) with (4), are time-discrete approximations for the semidiscrete process (12), since all modifications vanish as  $\Delta t$  goes to zero.

## 4 Conclusive remarks

We have analysed in depth the staircasing phenomenon in a semidiscrete setting. By use of numerical tests, we have validated the theoretical results and discussed important properties of semidiscrete and fully discrete schemes for SILD processes. The results obtained in this paper are important as a theoretical foundation for the optimal design of discrete sharpening processes in image processing as well as in the context of FCT schemes.

## Acknowledgements

The authors want to acknowledge the financial support of their works by Deutsche Forschungsgemeinschaft (DFG) under grants no. SO 363/9-1 and WE 3563/2-1, respectively. The second author also wants to express his thanks to the Dept. of Mathematics and Computer Science, Emory University, Atlanta, and the Institute for Mathematics and its Applications, University of Minnesota, Minneapolis, for their hospitality.

## References

- [1] J.P. Boris and D.L. Book (1973): Flux-Corrected Transport I: SHASTA, a fluid-transport algorithm that works. *Journal of Computational Physics*, 11:38–69
- [2] M. Breuß (2006): An analysis of discretisations of inverse diffusion equations. *Computing Letters*, to appear
- [3] A. Buades, B. Coll and J.M. Morel (2005): Neighborhood Filters and PDE's. CMLA Preprint 2005-04, ENS Cachan
- [4] A. F. Filippov (1988): *Differential Equations with Discontinuous Right-hand Sides*. Kluwer, Dordrecht
- [5] G. Gilboa, N. Sochen and Y. Y. Zeevi (2002): Forward-and-backward diffusion processes for adaptive image enhancement and denoising. *IEEE Transactions on Image Processing*, 11(7):689–703
- [6] S. L. Keeling and R. Stollberger (2002): Nonlinear anisotropic diffusion filters for wide range edge sharpening. *Inverse Problems*, 18:175–190
- [7] D. Kuzmin, R. Löhner and S. Turek, editors (2005): *Flux-Corrected Transport*. Springer
- [8] P.G. LeFloch and J.-G. Liu (1999): Generalized Monotone Schemes, Discrete Paths of Extrema, and Discrete Entropy Conditions. *Math. Comp.*, 68(227):1025–1055
- [9] R. J. LeVeque (2002): *Finite Volume Methods for Hyperbolic Problems*. Cambridge University Press
- [10] S. Levine, Y. Chen and J. Stanich (2004): Image Restoration via Non-standard Diffusion. Technical Report 04-01, Dept. of Mathematics and Computer Science, Duquesne University, Pittsburgh



- [11] S. Osher and L. Rudin (1991): Shocks and other nonlinear filtering applied to image processing. In A.G. Tescher, editor, *Applications of Digital Image Processing (XIV)*, volume 1567 of *Proceedings of the SPIE*, 414–431. SPIE Press, Bellingham
- [12] P. Perona and J. Malik (1990): Scale-space and edge detection using anisotropic diffusion. *IEEE Transactions on Pattern Analysis and Machine Intelligence*, 12(7):629–639
- [13] I. Pollak, A.S. Willsky and H. Krim (1997): Scale space analysis by stabilized inverse diffusion equations. In B. ter Haar Romeny, L. Florack, J. Koenderink, M. Viergever, editors, *Scale-Space Theory in Computer Vision*, volume 1252 of *Lecture Notes in Computer Science*, 200–211. Springer, Berlin
- [14] I. Pollak, A.S. Willsky and H. Krim (2000): Image segmentation and edge enhancement with stabilized inverse diffusion equations. *IEEE Transactions on Image Processing*, 9(2):256–266
- [15] G. Steidl, J. Weickert, T. Brox, P. Mrázek and M. Welk (2004): On the equivalence of soft wavelet shrinkage, total variation diffusion, total variation regularization, and SIDes. *SIAM Journal on Numerical Analysis*, 42(2):686–713
- [16] J. Weickert and B. Benhamouda (1997): A semidiscrete nonlinear scale-space theory and its relation to the Perona–Malik paradox. In F. Solina, W.G. Kropatsch, R. Klette, R. Baicsy, editors, *Advances in Computer Vision*, 1–10. Springer, Wien
- [17] M. Welk and J. Weickert (2005): Semidiscrete and discrete well-posedness of shock filtering. In C. Ronse, L. Najman, E. Decencièrè, editors, *Mathematical Morphology: 40 Years On*, volume 30 of *Computational Imaging and Vision*, 311–320. Springer, Dordrecht
- [18] M. Welk, J. Weickert and I. Galić (2005): *Theoretical Foundations for 1-D Shock Filtering*. Technical Report No. 150, Department of Mathematics, Saarland University, Saarbrücken, Germany, submitted
- [19] R.T. Whitaker and S.M. Pizer (1993): A multi-scale approach to nonuniform diffusion. *CVGIP: Image Understanding*, 57:99–110